AIP | Review of Scientific Instruments

Contributed Review: Distributed optical fibre dynamic strain sensing

Ali Masoudi and Trevor P. Newson

Citation: Review of Scientific Instruments **87**, 011501 (2016); doi: 10.1063/1.4939482
View online: http://dx.doi.org/10.1063/1.4939482
View Table of Contents: http://scitation.aip.org/content/aip/journal/rsi/87/1?ver=pdfcov
Published by the AIP Publishing

REVIEW OF SCIENTIFIC INSTRUMENTS **87**, 011501 (2016)

Contributed Review: Distributed optical fibre dynamic strain sensing

Ali Masoudi[a] and Trevor P. Newson
Optoelectronics Research Centre, University of Southampton, Hampshire SO17 1BJ, United Kingdom

(Received 13 September 2015; accepted 12 December 2015; published online 8 January 2016)

Extensive research on Brillouin- and Raman-based distributed optical fibre sensors over the past two decades has resulted in the commercialization of distributed sensors capable of measuring static and quasi-static phenomena such as temperature and strain. Recently, the focus has been shifted towards developing distributed sensors for measurement of dynamic phenomena such as dynamic strain and sound waves. This article reviews the current state of the art distributed optical fibre sensors capable of quantifying dynamic vibrations. The most important aspect of Rayleigh and Brillouin scattering processes which have been used for distributed dynamic measurement are studied. The principle of the sensing techniques used to measure dynamic perturbations are analyzed followed by a case study of the most recent advances in this field. It is shown that the Rayleigh-based sensors have longer sensing range and higher frequency range, but their spatial resolution is limited to 1 m. On the other hand, the Brillouin-based sensors have shown a higher spatial resolution, but relatively lower frequency and sensing ranges. © *2016 AIP Publishing LLC.* [http://dx.doi.org/10.1063/1.4939482]

I. INTRODUCTION

Today, sensors play an increasingly important role in various aspects of human life. Amongst the various types of sensing mechanisms, optical fibre sensors (OFSs) have attracted a considerable amount of attention due to the advantages they offer such as robustness, flexibility, and high sensitivity. In spite of these advantages, most single point OFS are typically one to two orders of magnitude more expensive than their electronic counterparts due to high manufacturing and components costs.[1] Unlike single point OFS, distributed optical fibre sensors (DOFSs) are not only robust and flexible but also cost-effective, thanks to their unique sensing mechanism. DOFS rely on a single set of optical components to interrogate and spatially resolve measurands along an optical fibre. In this way, tens of thousands of point sensors can be effectively replaced by a DOFS comprised of a single sensing fibre, a light source, and a detector.[2]

For more than two decades, the majority of studies on DOFS have focused on measuring the absolute temperature and strain along the sensing fibre using inelastic scattering processes i.e., Brillouin and Raman scattering. High sensitivity, simplicity, and the long sensing-range of Brillouin- and Raman-based DOFS have established them as the primary means for long-range temperature and strain measurement and have led to commercialization of these systems.[3] In recent years, research and investment in developing a new class of distributed sensors capable of detecting dynamic phenomena such as dynamic vibrations and sound waves have accelerated. The main driving force behind the expansion of this field has been the growing demand in areas such as the oil and gas industries, geophysical sciences, and structural health monitoring.

[a]Electronic mail: a.masoudi@soton.ac.uk

Distributed optical fibre dynamic strain sensors can be broadly divided into two categories: (1) DOFS capable of detecting dynamic perturbations[4–6] and (2) DOFS capable of both detecting and quantifying dynamic perturbations. The focus of this review is to study the sensors which fall into the second category.

This article begins with a brief analysis of the principles of the two light scattering phenomena which have been used in distributed dynamic sensors in Section II. Sections III and IV study the distributed dynamic strain sensing techniques. The principle of each technique is elucidated followed by a case study of the most recent advances in that technique. Finally, in Section V, different sensing techniques are compared and their advantages and disadvantages are summarized.

II. PRINCIPLES OF LIGHT SCATTERING

Light scattering is a consequence of the interaction between an incident electromagnetic (EM) wave and atoms or molecules of a medium. Light scatters through three different processes: Rayleigh, Brillouin, and Raman. Of the three scattering processes, only Rayleigh and Brillouin scattering are influenced by the strain of the medium. This section describes the principle of these two scattering processes.

A. Rayleigh scattering

When an EM wave encounters density fluctuations in an otherwise homogeneous medium, it periodically perturbs the electron cloud of the molecules within the medium. The oscillation of the electron cloud results in a periodic polarization of atoms or molecules in that region which forms an oscillating dipole moment. The oscillation of the induced dipole moment leads to the radiation of a secondary EM wave known as Rayleigh scattering. It is shown that the sum of the secondary waves radiated from a perfectly homogeneous medium is zero in all directions except in the

direction of the propagation of the incident wave.[7] Therefore, the Rayleigh scattering phenomenon is only observed in an inhomogeneous medium. Since the induced dipole moments oscillate at the frequency of the incident wave, the wavelength of the Rayleigh scattered light is identical to that of the incident wave. Therefore, Rayleigh scattering is an elastic process.

Rayleigh scattering occurs due to randomly distributed density fluctuations in the fibre. These inhomogeneities, which in size are much smaller than the wavelength of the propagating light, form during the fibre fabrication process. The ratio of the intensity of the scattered light to that of the incident light is known as the Rayleigh scattering coefficient which, for a condensed isotropic media, is given by[8,9]

$$\gamma_R = \frac{8\pi^3}{3\lambda^4} n^8 p^2 \beta_T K T_F. \quad (1)$$

In this equation, λ is the wavelength of the incident light. The description of the rest of the parameters and their values for a standard SMF-28 optical fibre is given in Table I.

It should be noted that the sensing principle of the Rayleigh-based OFS depends almost entirely on these inhomogeneities and their relative movements. Any fluctuation in the position of these inhomogeneities due to variations in temperature and strain of the fibre affects the phase, intensity and polarization of the Rayleigh scattered light in the fibre. These variations, in turn, are used to map those physical parameters.

B. Brillouin scattering

Brillouin scattering occurs as a result of the interaction between incident light and thermally generated acoustic phonons. Acoustic phonons are quantized vibrational modes of atoms or molecules in condensed matter. Therefore, they can be considered as thermally generated acoustic waves propagating in all directions over a wide range of frequencies. Consequently, Brillouin scattering can be modeled as the diffraction of light due to periodic variations in the refractive index of a medium caused by thermally generated acoustic waves.

Brillouin scattering in an optical fibre follows a similar principle. As light travels through the fibre, it interacts with the thermally generated acoustic phonons. Of all the phonons in the fibre, only those which are phase-matched with the incident wave (i.e., those which satisfy the Bragg condition) contribute to the Brillouin scattering process. The wavelength of the scattered light which satisfies the Bragg condition is given by[10]

TABLE I. Definition of the parameters in Equation (1) along with their values for a SMF-28 optical fibre.

Symbol	Description	Value
n	Fibre refractive index	1.46
p	Average photoelastic coefficient	0.286
β_T	Isothermal compressibility at T_F	7×10^{-11} m^2 N^{-1}
K	Boltzmann constant	1.38×10^{-23} J K^{-1}
T_F	Fictive temperature	1950 K

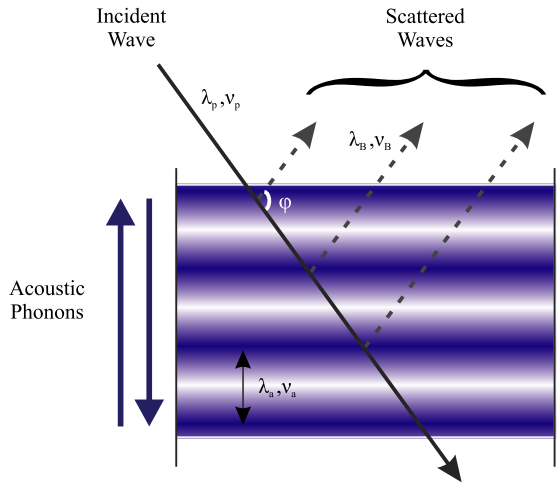

FIG. 1. Brillouin scattering (λ_B) as a result of interaction between an incident light (λ_P) and thermally generated acoustic waves (λ_a).[10]

$$\lambda_p = 2n\,\lambda_a \sin(\frac{\varphi}{2}), \quad (2)$$

where n is the refractive index of the fibre, λ_a is the wavelength of the acoustic wave, and φ is the angle between the incident and scattered light. Figure 1 illustrates the process of Brillouin scattering for an acoustic wave propagating parallel to the waveguide. Only scattered rays within the numerical aperture (NA) of the fibre are guided by the fibre. Therefore, the acoustic phonons propagating in parallel with the axis of the fibre contribute most towards the backscattered light detected at the front-end of the fibre.

As a result of the interaction of light with the acoustic phonons travelling at the velocity υ_a, the scattered light undergoes a Doppler shift. The frequency of the acoustic phonons, f_a, can be expressed in terms of its velocity, υ_a, and its wavelength as

$$f_a = \frac{\upsilon_a}{\lambda_a}. \quad (3)$$

Combining Equations (2) and (3) gives

$$f_a = \frac{2n}{\lambda_P} \upsilon_a \sin(\frac{\varphi}{2}). \quad (4)$$

This equation demonstrates the frequency of the phonons in terms of the wavelength of the incident light and the refractive index of the fibre. The frequency difference between the incident and scattered light, which is called the Brillouin frequency shift, $\Delta\nu_B$, is equal to the frequency of the acoustic wave, f_a. Since only the scattered light in the forward and backward directions are guided (i.e., $\varphi = 0°$ and $\varphi = 180°$), the frequency shift of the Brillouin backscattered light is

$$|\nu_p - \nu_{BS}| = |\Delta\nu_B| = \frac{2n}{\lambda_P} \upsilon_a, \quad (5)$$

where ν_p and ν_{BS} are the frequencies of the incident and backscattered light, respectively. The sign of the Brillouin frequency shift depends on the direction of the acoustic wave with respect to that of the incident light. The Brillouin scattering with the frequency down-shifted or longer wavelength is referred to as Stokes backscattered light while the Brillouin

scattering with the frequency up-shifted or shorter wavelength is referred to as anti-Stokes backscattered light.

Equation (5) shows that, for a given incident wavelength, the Brillouin frequency shift depends on the refractive index of the fibre and the acoustic velocity within the fibre. In turn, both of these parameters are dependent on the temperature and strain in the fibre. The intensity of the Brillouin backscattered light is also dependent on the temperature and strain in the fibre. The Brillouin scattering coefficient, γ_B, is given by[8]

$$\gamma_B = \frac{8\pi^3}{3\lambda^4} n^8 p^2 K T (\rho \upsilon_a^2)^{-1}, \tag{6}$$

where T is the absolute temperature and ρ is the mean density of the fibre. Therefore, by analyzing the intensity and frequency of the Brillouin backscattered light, the strain and temperature distribution along the sensing fibre can be unambiguously measured.[11]

Unlike Rayleigh, Brillouin scattering can be optically stimulated to enhance the intensity of the Brillouin backscattered light. At low pump power, the intensity of the spontaneous Brillouin scattering is proportional to the intensity of the pump light. As the power of the pump light increases, the intensity of the Stokes wave grows by the process of electrostriction. The interaction between the pump light and the backscattered Stokes light forms a forward propagating refractive index grating.[12] This forward propagating grating, in turn, increases the Brillouin Stokes power. Increasing the intensity of the pump light beyond the threshold level P_{th} results in a significant modification in the local refractive index which, in turn, causes a large proportion of the pump power to be transferred to the backward propagating Stokes Brillouin beam. This process which is known as stimulated Brillouin scattering (SBS) can be used to enhance the Brillouin backscattered light.

C. Comparison

Considering the differences in the nature of the Rayleigh and Brillouin scattering processes, a comparison between the two processes can provide a valuable insight into the capabilities and limitations of DOFS using them. The intensity of spontaneous Brillouin scattering for each of Stokes and anti-Stokes lines are ~18 *dB* lower than that of the Rayleigh scattering. Therefore, DOFSs which are based on spontaneous Brillouin scattering require a large amount of averaging to achieve a reasonable signal to noise ratio (SNR). As a result, most of the Brillouin-based DOFSs are developed as quasi-static distributed temperature/strain sensors.

The difference in the sensing mechanism is another significant aspect which distinguishes the two sensing regimes. Brillouin-based DOFS use the frequency and intensity variations of the Brillouin backscattered light to measure the absolute temperature and strain of the fibre. The measurement of the absolute temperature and strain is feasible due to the linear relationship between the energy of the acoustic phonons and the temperature and strain of the fibre. Rayleigh-based DOFS, on the other hand, are capable of measuring only the relative changes in the measurands along the sensing fibre. This is due to the fact that the sensing procedure of these sensors rely on the relative motion of the inhomogeneities in the sensing fibre. Therefore, distributed sensors which rely on Rayleigh backscattered light cannot be used to measure the absolute value of a physical entity.

III. DISTRIBUTED DYNAMIC STRAIN SENSORS BASED ON RAYLEIGH SCATTERING

A. Optical time domain reflectometry (OTDR)

OTDR is the simplest form of fibre interrogation technique. This technique was first used by Barnoski and Jensen[13] as a mean to investigate the attenuation characteristics along a 360 m long optical fibre. The principle of this technique is based on launching a pulse of light down one end of the sensing fibre and collecting the backscattered Rayleigh light from the same end. The round trip of the light pulse in the fibre results in a trace at the front-end of the fibre where each point on the trace represents one section of the fibre. Hartog and Gold[14] have shown that for an optical pulse with a peak intensity of I_0, the intensity of the backscattered light at the front-end of the fibre is given by

$$I_R(x) = \frac{1}{2} v_g I_0 t_p S \gamma_R \exp(-2\gamma x), \tag{7}$$

where $x = t\, v_g/2$ is the distance from the front-end and S is the capture fraction. Using the mathematical analysis and the diagrams, the value of S can be written as[14]

$$S = \frac{1}{4.3} \frac{(NA)^2}{n^2}. \tag{8}$$

The description of the elements in Equations (7) and (8) and their typical values at 1550 nm are given in Table II.

DOFSs which use the Rayleigh backscattered light in an OTDR setup to interrogate the sensing fibre fall into three categories including correlation-OTDR (COTDR), polarization-OTDR (POTDR), and phase-OTDR (φ-OTDR). Although all three techniques have been used to detect dynamic perturbations,[4–6] thus far, only systems based on φ-OTDR have demonstrated the capability of quantifying the perturbations.

The underlying principle of φ-OTDR sensors is based on monitoring the phase of the Rayleigh backscattered light along the sensing fibre. For any given section on the sensing fibre, the phase-difference between the backscattered light from the two ends of that section is a linear function of the length of the section. Therefore, by monitoring the variation in the phase-difference of the backscattered light from the two ends of each section, strain on that section of the fibre can be quantified.

TABLE II. The description and typical values of the elements of Equations (7) and (8) for step index standard SMF-28 fibre.

Symbol	Description	Value
v_g	Group velocity	$\sim 2\times10^8$ m s^{-1}
t_p	Pulse width	...
S	Capture fraction	2.11×10^{-3}
γ_R	Rayleigh scattering coefficient	4.6×10^{-5} m^{-1}
γ	Attenuation coefficient	$\sim 4.6\times10^{-5}$ m^{-1}
NA	Numerical aperture	0.14
n	Fibre refractive index	1.46

Using φ-OTDR as a distributed vibration sensor (DVS) was first proposed by Dakin and Lamb.[15] In the proposed setup, a pair of pulses with slightly different frequency (f_1 and f_2) is launched separately into the sensing fibre (Figure 2(a)). The temporal separation between the two pulses results in the backscattered light from the first pulse at location x_1 to be mixed with the backscattered light from the second pulse at location x_2, with the spatial separation between x_1 and x_2 is $\Delta x = \Delta T \cdot c/2n$. In this equation, ΔT is the temporal separation between the two pulses and c is the speed of light in vacuum. The combination of the two backscattered traces at the photodetector results in a signal with a beat frequency of $\Delta f = |f_1 - f_2|$. Dakin and Lamb showed that the phase of the beat signal for any given section of the fibre has a linear relationship with the strain of that section. Although, in theory, the proposed concept can provide the phase information along the sensing fibre, in practice, for the setup to work, a precise control over the phase of the two interrogating pulses is required. This concept was later adopted and modified by Lewis and Russell[16,17] to propose a DVS capable of measuring the vibrations along the sensing fibre. In 2014, Alekseev *et al.*[18] experimentally demonstrated this concept by controlling the relative phase of a dual-pulse probe signal. The experimental results showed that this sensing technique is capable of measuring 230 Hz periodic perturbations along a 2 km long sensing fibre with a spatial resolution of 5 m and a phase sensitivity of 0.01 rad.

In the year 2000, Posey *et al.*[19] demonstrated an alternative measurement technique in which the relative phase of the backscattered light between two separate sections in the sensing fibre was measured using an imbalanced Mach-Zehnder interferometer (MZI) (Figure 2(b)). In their technique, the backscattered light from a single pulse is inserted into an imbalanced MZI with two unequal arms to provide two similar traces with temporal shift of $\Delta T = \Delta L \cdot n/c$, where ΔL is the path imbalance of the MZI. Afterward, the two traces are mixed in a 3×3 coupler to provide three electromagnetic waves with a nominal phase-shift of 120° between them. Finally, the differential phase information at one section of the sensing fibre (the red dot on the train of the backscattered traces in Figure 3(a), for instance) can be extracted by gating the backscattered signals from that section and demodulating the signal using a phase-demodulator. This sensing technique was used to measure 2 kHz dynamic strain in the middle of a 400 m long sensing fibre by slowly scanning the entire length of the fibre.

Posey's dynamic measurement technique was later developed independently by both Masoudi *et al.*[20,21] and Farhadiroushan *et al.*[22] to realize DVS systems capable of mapping the vibrations along the entire length of the sensing fibre simultaneously. The experimental setups described in these publications are both similar to that of the Posey. In this technique, to measure the dynamic variations, the acquired data can be differentiated either as a function of time (temporal derivation or derivation along the slow axis) or as a function of distance (spatial derivation or derivation

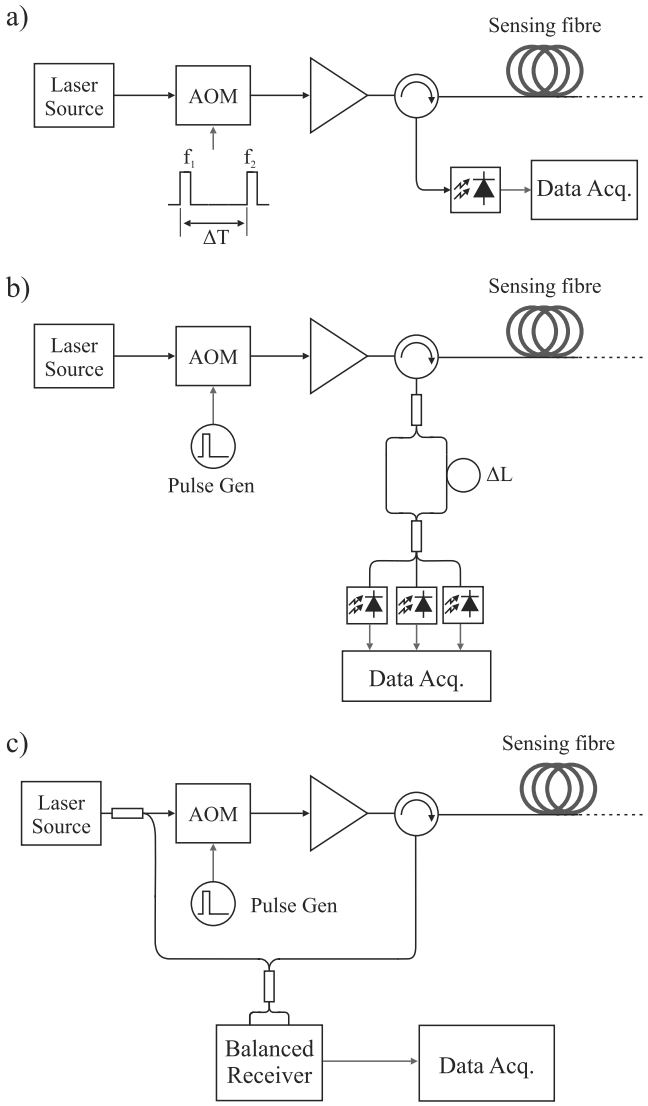

FIG. 2. The outline of the experimental setups of three DVS, the operations of which are based on φ-OTDR.

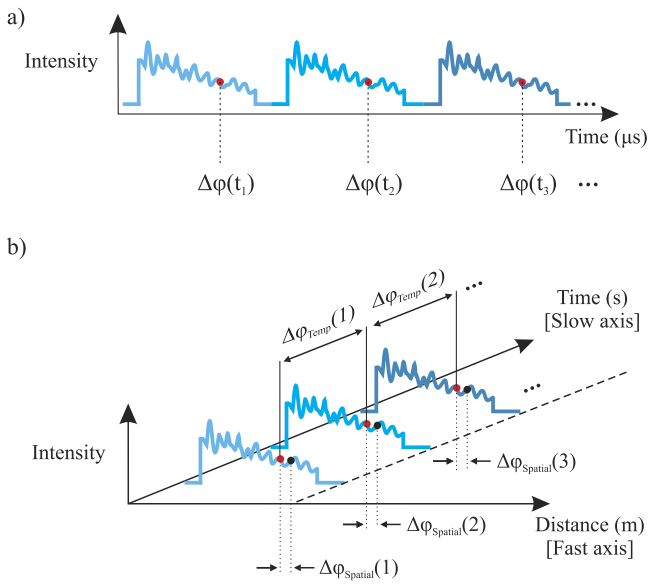

FIG. 3. The sensing principle of interferometric φ-OTDR sensor based on 3×3 coupler using (a) signal gating measurement technique and (b) distributed measurement technique.

along the fast axis) (Figure 3(b)). The schematic of the signal processing procedure disclosed in Farhadiroushan *et al.* patent suggests that since the outputs of the detectors are directly fed to the phase-detection unit, their sensing technique relies on the spatial-derivative of the backscattered data to measure the perturbations. Masoudi *et al.* setup, on the other hand, quantifies the vibrations by measuring temporal-derivative of the acquired data using a computer algorithm. Using this φ-OTDR sensing technique, Masoudi *et al.*[20,21] demonstrated a 1 km long distributed vibration sensor with a strain and frequency range of 2 $\mu\varepsilon$ and 4000 Hz, respectively. The spatial resolution of the sensor was measured to be 1 m.

Another technique, proposed by Hartog and Kader,[23] is based on converting the data from the optical domain to the electrical domain before measuring the phase difference in the electrical domain (Figure 2(c)). In this approach, an AOM is used to generate optical pulses with a frequency shift of Δf relative to the light source. The backscattered light from the fibre is mixed with the light source at a balanced photodetector to generate a beat signal which retains both the amplitude and phase information. The phase information along the fibre is then measured in the electrical domain using a phase detection circuit. The experimental results, demonstrated by Tu *et al.*,[24] showed that this sensing technique is capable of spatially resolving 80 Hz dynamic strains along 25 km of sensing fibre with a spatial resolution of 10 m and a strain range of 400 $n\varepsilon$.

Another technique, proposed by Hartog and Kader,[23] is based on converting the data from the optical domain to the electrical domain before measuring the phase difference in the electrical domain (Figure 2(c)). In this approach, an acousto-optic modulator (AOM) is used to generate optical pulses with a frequency shift of Δf relative to the light source. The backscattered light from the fibre is mixed with the light source at a balanced photodetector to generate a beat signal which retains both the amplitude and phase information. The phase information along the fibre is then measured in the electrical domain using a phase detection circuit. The experimental results, demonstrated by Tu *et al.*,[24] showed that this sensing technique is capable of spatially resolving 80 Hz dynamic strains along 25 km of sensing fibre with a spatial resolution of 10 m and a strain range of 400 $n\varepsilon$.

The main limitation of φ-OTDR sensing technique is the linearity of its responses.[25] Since the measured strain at each section of the sensing fibre is based on the relative phase at the two ends of that section, the intrinsic phases of those ends play an important role in the linearity of the response. If the distribution of the inhomogeneities of the two ends is not affected by the strain, the strain between the two ends would have a linear relationship with the phase. However, any perturbation in the distribution of inhomogeneities at the two ends results in a non-linear response between the strain and the measured phase.

The φ-OTDR sensing technique may also suffer from signal fading. The Rayleigh backscattered signal from each section of the sensing fibre is formed by the addition of the backscattered photons from randomly distributed scattering centres within the scattering zone with arbitrary phases. For a highly coherent light, this addition leads to significant fluctuations in the power of the backscattered light which may cumulate to near zero and, hence, fading of signal. This problem can be eliminated either by using multiple interrogation frequencies to probe the sensing fibre or by using a relatively broadband light source.

It should be noted that the term φ-OTDR is also used to describe OTDRs which use coherent sources and homodyne detection to measure the intensity of the backscattered traces.[6,26] In this technique, the backscattered light is mixed with the laser source to extract the absolute phase of the backscattered light relative to the light source and this is used to detect perturbation along the fibre. In the current sub-section, however, the term φ-OTDR is used to describe the systems which use the phase-difference between two adjacent sections of the sensing fibre rather than the absolute phase of the backscattered light.

B. Optical frequency domain reflectometry (OFDR)

The principle of OFDR interrogation technique, first introduced by Eickhoff and Ulrich,[27] is based on mapping the fibre as a function of the frequency of the backscattered light. In this technique, a monochromatic light source is used as the probe light while its optical frequency is linearly swept. To spatially resolve the backscattered data along the fibre, the backscattered light is mixed with the light source to generate a range of beat signals at the detector. Each beat frequency correspond to the backscattered light from a certain section of the sensing fibre. The signals with smaller beat frequency correspond to the backscattered light from sections closer to front-end of the sensing fibre while the signals with larger beat frequency correspond to the backscattered light from the sections of the fibre closer to the far-end of the fibre. By computing the fast Fourier transform (FFT) of the acquired data at the detector and resolving the frequency components of the mixed signals, the backscattered light along of the sensing fibre can be spatially resolved. Figure 4 shows the generic layout of such a setup.

The relationship between the beat frequency, Ω, and the distance from the front-end of the fibre, x, is given by[27]

$$\Omega = \frac{2x}{v_g}\frac{d\omega}{dt}, \tag{9}$$

where v_g is the group velocity of the fibre and $d\omega/dt$ is the sweeping rate of the wavelength (optical frequency) of the laser source.

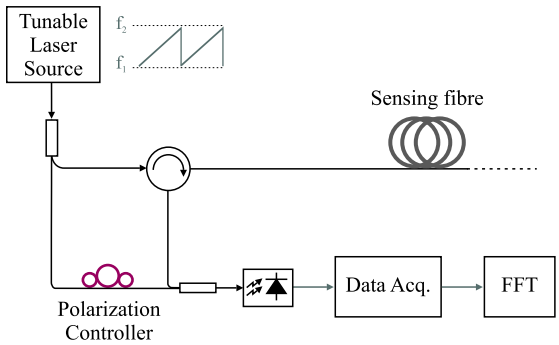

FIG. 4. The generic layout of an optical frequency-domain reflectometry (OFDR) setup.

OFDR was initially developed as a high-spatial-resolution loss measurement technique for waveguides and optical fibres. Froggatt and Moore[28] was the first to demonstrate a distributed strain sensor using OFDR interrogation technique. In this technique, OFDR is used to map the spatial-distribution of inhomogeneities along the sensing fibre. Since an induced strain on the fibre shifts the position of the inhomogeneities, the strain rate on the fibre can be measured using the cross correlation between OFDR traces. In 2012, Zhou *et al.*[29] used this interrogation technique to measure dynamic strains up to 20 Hz along 10 m of sensing fibre with an spatial resolution of 10 cm.

The drawback of strain measurement through cross correlation analysis of the OFDR traces is its limited strain range. This is due to the fact that the pattern of the OFDR backscattered traces depends on the spatial distribution of the inhomogeneities in the sensing fibre. Applying strain to the fibre not only shifts in the position of the inhomogeneities but also results in redistribution of them. Since the cross correlation data analysis requires the data to be relatively uniform, any redistribution of inhomogeneities that alter the pattern of the OFDR traces appears as noise. Therefore, the operation of this sensing technique is limited to a relatively small strain range between 0.1 and $\mu\varepsilon$ for which the pattern of the OFDR traces are relatively uniform.

IV. DISTRIBUTED DYNAMIC STRAIN SENSORS BASED ON BRILLOUIN SCATTERING

A. Brillouin optical time domain reflectometry (BOTDR)

The operation of BOTDR sensing technique is similar to that of OTDR described in Subsection III A except BOTDR interrogation relies on the spontaneous Brillouin backscattered light. BOTDR is the simplest Brillouin-based interrogation technique in which the wavelength and intensity of the spontaneous Brillouin backscattered signal are used to map the temperature and strain along the fibre.[30] The intensity of the Brillouin backscattered light at the front-end of the fibre is given by

$$I_B(x) = \frac{1}{2} v_g I_0 t_p S \gamma_B \exp(-2\gamma x), \tag{10}$$

where γ_B is the Brillouin scattering coefficient. The description of the other elements in this equation is given in Table II. The typical value of the Brillouin scattering coefficient for silica based fibre is $\gamma_B \cong 1.17 \times 10^{-6}\ \mathrm{m}^{-1}$. Figure 5 shows the generic layout of a BOTDR setup.

As mentioned earlier, Brillouin-based DOFSs are traditionally limited to static measurements since: (1) the backscattered light due to Brillouin scattering process is very weak and, as a result, any measurement relies on a large number of averages, and (2) measuring the Brillouin gain spectrum (BGS) is a slow process which relies on scanning the Brillouin gain spectrum using a microwave detector.[31] Due to these limitations, BOTDR-based dynamic strain sensors have limited frequency range. Wang *et al.*[32] demonstrated such a system with a maximum detectable frequency of 11 Hz over 4 km of sensing fibre. However, the proposed setup had a poor strain sensitivity of 100 $\mu\varepsilon$ with a spatial resolution of 10 m.

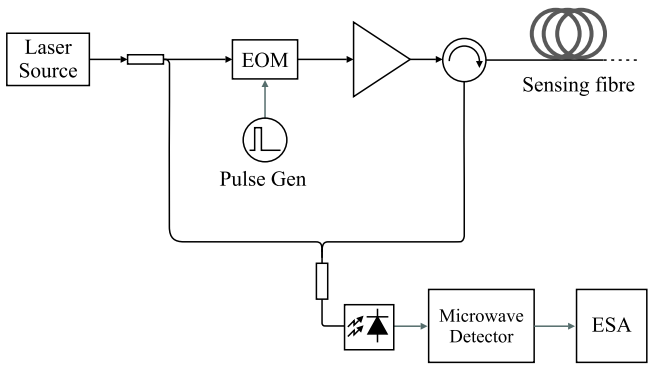

FIG. 5. The generic layout of a Brillouin optical time domain reflectometry (BOTDR) setup.

To overcome the slow mapping process of the BGS, Masoudi *et al.*[33] proposed a technique to convert the changes in the frequency of the Brillouin backscattered light to intensity variation. In this technique, an imbalanced MZI is employed to convert the Brillouin frequency shift to optical intensity variations at the photodetector. The proposed sensor demonstrated a strain sensitivity of 50 $\mu\varepsilon$ over 2 km of sensing fibre with a spatial resolution of 1.3 m. However, with a sampling rate of 2 Sa/s, the described system had a maximum detectable frequency of 1 Hz.

B. Brillouin optical time domain analysis (BOTDA)

BOTDA is a more complex form of BOTDR which relies on stimulated Brillouin scattering. In this technique, an optical pulse and CW light with a frequency difference equivalent to the Brillouin frequency shift are launched at two opposite ends of the sensing fibre as shown in Figure 6. The interaction between these two waves at the segments of the sensing fibre which meet the Bragg condition results in SBS. The stimulated scattering process results in a more intense Brillouin scattering which, consequently, requires less averaging to achieve a reasonable SNR. By scanning the wavelength of either the

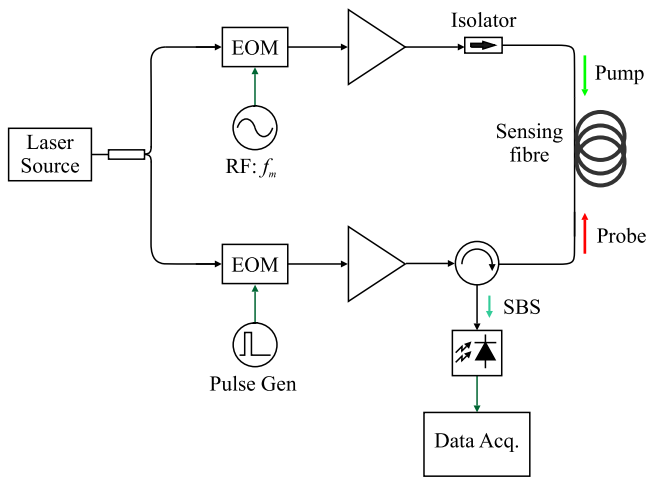

FIG. 6. The generic layout of a Brillouin Optical Time Domain Analysis (BOTDA) setup.

CW light or the optical pulse over the BFS, the temperature and strain along the sensing fibre can be mapped.[34]

Brown *et al.*[35] reported the first experimental results on BOTDA-based distributed optical fibre dynamic strain sensor. The sensing procedure of the proposed setup is based on separately launching several probe pulses at different frequencies into the sensing fibre and forming the Brillouin gain profile. Despite a sampling rate of 2 kHz, the spatial and strain resolution of the sensor was limited to 12 m and 200 $\mu\varepsilon$, respectively, over 120 m sensing range. Since this technique requires the frequency difference between the probe and pump signal to be stepped through the Brillouin frequency shifts range to form the BGS, it is very slow and, hence, not suitable for dynamic measurement.

In order to increase the frequency range of BOTDA-based techniques, two different sensing procedures were proposed: Slope-Assisted BOTDA (SA-BOTDA) and Brillouin Phase-Shift OTDA (BPS-OTDA). SA-BOTDA was first introduced by Bernini *et al.*[36] This technique requires a preliminary Brillouin frequency scan in order to map the Brillouin frequency shift distribution along the sensing fibre using conventional BOTDA technique. After this step, the optical frequency difference between the probe pulse and the counter-propagating CW light is fixed in order to form a BGS with its quadrature point sitting at the Brillouin frequency shift of the sensing fibre. Therefore, the BGS effectively acts as a frequency discriminator which converts variations in the Brillouin frequency shift (BFS) to changes in the optical power. Using this technique, Bernini *et al.*[36] demonstrated a dynamic strain sensor with 200 Hz bandwidth capable of detecting strains as low as 95 $\mu\varepsilon$ over 30 m of sensing fibre with a spatial resolution of 3 m.

The strain range of the SA-BOTDA technique demonstrated by Bernini *et al.*, however, is limited to less than half the Brillouin gain spectrum linewidth and cannot be implemented if there are larger variations in the BFS along the sensing fibre. Peled *et al.*[37] introduced an alternative method to solve this problem by adjusting the optical frequency of the pump. Similar to Bernini's approach, this technique also requires the BGS along the sensing fibre to be initially mapped using conventional BOTDA technique. This slow mapping phase is followed by a fast interrogation phase in which the frequency of the pump light is adjusted with regards to the local BFS so that when the probe wave meets the counter-propagating pump, the optical frequency difference between the pump and the probe light sits at the quadrature point of the BGS slope (Figure 7). Using this technique, Peled *et al.*[37] have demonstrated an 85 m long distributed sensor with a frequency and a dynamic range of 400 Hz and 600 $\mu\varepsilon$, respectively.

In 2012, an alternative interrogation technique was introduced which, unlike the SA-BOTDA, was not sensitive to the variations in the amplitude of the detected probe wave. In this technique, the dynamic strain is measured using the variation in the Brillouin phase-shift instead of the intensity of the Brillouin backscattered light.[38] To realize this technique, the Brillouin probe wave is phase-modulated to generate two side-bands. The frequency of the phase-modulation is selected in such a way that only the upper side-band of the probe wave interacts with the pump wave. The analysis of the upper side-band shows that its phase is dependent on the Brillouin frequency shift, but independent of the line shape of the BGS. By isolating the phase of the upper side-band using a phase-demodulator and monitoring the modulation frequency and modulation amplitude, the dynamic strain along the sensing fibre can be mapped. Using this sensing technique, Urricelqui *et al.*[38] demonstrated a distributed dynamic strain sensor with an effective sampling rate of 1.6 kHz and a spatial resolution of 1 m over a sensing range of 160 m.

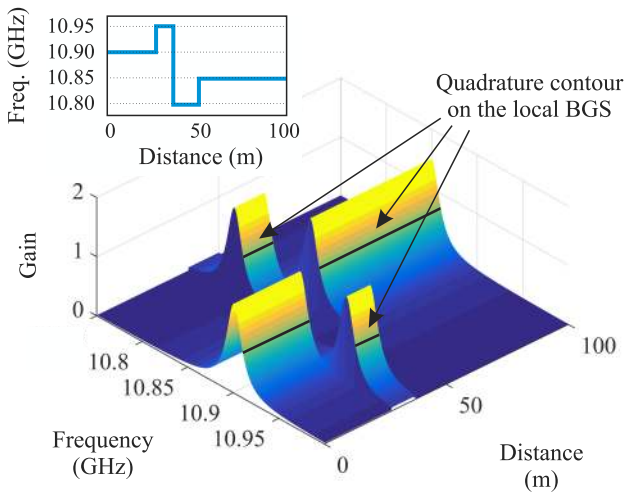

FIG. 7. An example of the local Brillouin gain spectrum (BGS) as a function of Brillouin frequency shift and distance along a sensing fiber.[37]

The BOTDA sensing technique, however, suffers from two main drawbacks. One of the problems may arise from a slow but continuous variation in the temperature and strain of the sensing fibre which may significantly affect the spectral shape of the Brillouin gain and the quadrature point on the local BGS. Therefore, any sensor which is based on the SA-BOTDA or BPS-OTDA interrogation techniques requires a constant BGS recalibration using the conventional BOTDA technique which is a slow and time consuming process.

On the other hand, the BOTDA sensing technique is best reserved for monitoring a single disturbance in the sensing fibre where the relative Brillouin frequency shift between the disturbed and undisturbed regions of the fibre is greater than the Brillouin linewidth. If not, the apparent Brillouin gain spectrum at a point from which the strain is computed is influenced by the strain distribution along the fibre. This effect, first identified by Horiguchi *et al.*[39] and later analyzed by Geinitz *et al.*,[40] is due to the potential transfer of power between the CW pump light and the counter-propagating interrogating pulse all along the fibre from the point where the pulse enters the fibre to the point of measurement. However, the transfer of power between the pump and the probe light is significant only for long range distributed measurement and can be neglected for short range DOFS.[41]

C. Brillouin optical correlation-domain analysis (BOCDA)

Of the three Brillouin-based interrogating techniques, BOCDA is the most complex one. The principle of this technique is based on modulating the frequency of two

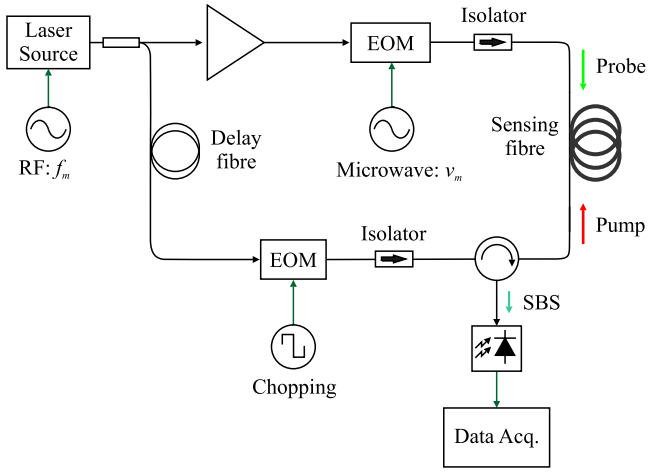

FIG. 8. The generic layout of a Brillouin Optical Correlation Domain Analysis (BOCDA) setup.

counter-propagating CW lights to invoke SBS at one section of the sensing fibre at any given time.[42] The point at which the two counter-propagating lights interact is controlled by adjusting the frequency at which the wavelength of the light sources is modulated. This sensing technique offers a number of unique features such as random accessibility of measuring position and high spatial resolution. Figure 8 shows the generic layout of a BOCDA setup in its simplest form.

After establishing the principle of BOCDA, Hotate *et al.* showed that this interrogation technique can be used to measure dynamic perturbations. In an article published in 2007, an experimental setup similar to the one shown in Figure 8 was used to measure sinusoidal strains at frequencies of up to 200 Hz along 20 m of sensing fibre and with a spatial resolution of 10 cm.[43] Using differential frequency modulation (DFM) technique in which the sensing position is periodically swept by applying slightly different modulation frequencies to the pump and the probe waves, a BOCDA-based interrogation system was demonstrated offering parameters such as a frequency range of 0–20 Hz and a strain accuracy of 50 $\mu\varepsilon$ over 100 m sensing range.[44] However, the underlying principles of the correlation technique pose a trade-off between the sensing range and the spatial resolution. Typically, the range is ~200 times the spatial resolution.

V. DISCUSSION & CONCLUSION

Detection and quantification of dynamic phenomena has opened a new frontier in distributed optical fibre research. DOFSs capable of quantifying dynamic vibrations fall into two categories: (1) Rayleigh-based sensors with long sensing and frequency range, but limited spatial resolution, and (2) Brillouin-based sensors with a relatively shorter gauge length, but superior spatial resolution and strain range. A summary of the main parameters of these two categories of sensors is presented in Table III. The higher scattering coefficient of Rayleigh scattering along with the interferometric sensing mechanism which relies on the phase of the backscattered light allows the Rayleigh-based DOFSs to demonstrate a long sensing range with a high strain resolution. This class of sensors are more suitable in areas such as geophysical sciences and structural health monitoring where the sensor is required to monitor minute strain variations over large distances. In addition, by optimizing the interferometric arrangement, the strain or spatial resolution of these sensors can be enhanced by at least two orders of magnitude. However, as mentioned earlier, this sensing technique does not provide the absolute strain, but rather the relative changes in the strain of the fibre.

Brillouin-based DOFSs, on the other hand, measure the absolute strain of the fibre using the Brillouin frequency shift. As a result, they are capable of measuring far larger strains with higher accuracy. However, Brillouin-based sensing techniques suffer from a negative trade-off between the frequency and sensing range. In addition, to achieve a reasonable SNR, most

TABLE III. Dynamic strain measurement: key parameters of the studies reported to date.

	Rayleigh				Brillouin				
	OTDR			OFDR [Ref. 29]	BOTDR [Ref. 33]	BOTDA			BOCDA [Ref. 44]
	3×3 coupler [Ref. 20]	Dual-pulse [Ref. 18]	Elec. Domain [Ref. 24]			Conventional [Ref. 35]	SA-BOTDA [Ref. 37]	BPS-OTDA [Ref. 38]	
Sensing Range (m)	1,000	25,000	2,000	10	1,000	120	85	160	~100
Frequency Range (Hz)	4,000	<100	<250	20	1	<2,000	400	800	20
Strain Range (με)	2	0.4	-	1	10×10^3	2.5×10^3	600	2560	650
Spatial Resolution (m)	1	10	5	0.1	1.3	12	1.5	1	0.8
Strain Resolution (με)	0.08	0.01	-	1	50	200	-	20	50
Sensing Mechanism	Relative Strain				Absolute Strain				

of the proposed techniques rely on 10–100 times averaging which significantly limits the frequency range of these sensor. Nevertheless, the main drawback of Brillouin-based DOFSs is their limited strain resolution which is determined by the bandwidth of the BGS. The best strain resolution for Brillouin-based dynamic strain sensor reported to date is 20 $\mu\varepsilon$, a value which can be reduced down to a minimum strain resolution of 1 $\mu\varepsilon$, but at the expense of the frequency range of the sensor.

[1]S. Krüger and W. Gessner, *Advanced Microsystems for Automotive Applications 2000* (Springer, Germany, 2000), pp. 111–112.
[2]M. N. Alahbabi, Y. T. Cho, and T. P. Newson, Meas. Sci. Technol. **17**, 1082 (2006).
[3]G. Bolognini and A. Hartog, Opt. Fiber Technol. **19**, 678 (2013).
[4]S. V. Shatalin, V. N. Treschikov, and A. J. Rogers, Appl. Opt. **37**, 5600 (1998).
[5]J. C. Juarez, E. W. Maier, N. C. Kyoo, and H. F. Taylor, J. Lightwave Technol. **23**, 2081 (2005).
[6]Y. Lu, T. Zhu, L. Chen, and X. Bao, J. Lightwave Technol. **28**, 3243 (2010).
[7]I. L. Fabelinskii, *Molecular Scattering of Light* (Springer, New York, 1968).
[8]J. Schroeder *et al.*, J. Am. Ceram. Soc. **56**, 510 (1973).
[9]R. Olshansky, Rev. Mod. Phys. **51**, 341 (1979).
[10]T. Still, Ph.D. thesis, Johannes Gutenberg–Universität Mainz, 2010.
[11]S. M. Maughan, H. H. Kee, and T. P. Newson, Meas. Sci. Technol. **12**, 834 (2001).
[12]A. Kobyakov, M. Sauer, and D. Chowdhury, Adv. Opt. Photonics **2**, 1 (2010).
[13]M. K. Barnoski and S. M. Jensen, Appl. Opt. **15**, 2112 (1976).
[14]A. Hartog and M. P. Gold, J. Lightwave Technol. **2**, 76 (1984).
[15]J. P. Dakin and C. Lamb, GB patent No. GB 2 222 247A (28 February 1990).
[16]A. B. Lewis and S. J. Russell, U.S. patent No. US 2012/0278043 A1 (1 November 2012).
[17]A. B. Lewis and S. J. Russell, U.S. patent No. US 2014/0204368 A1 (24 July 2014).
[18]A. E. Alekseev *et al.*, Laser Phys. **24**, 115106 (2014).
[19]R. Posey, G. A. Johnson, and S. T. Vohra, Electron. Lett. **36**, 1688 (2000).
[20]A. Masoudi, M. Belal, and T. P. Newson, Meas. Sci. Technol. **24**, 085204 (2013).
[21]A. Masoudi, M. Belal, and T. P. Newson, in *23rd International Conference on Optical Fibre Sensors* (Santander, Spain, 2014), p. 91573T.
[22]M. Farhadiroushan, T. R. Parker, and S. Shatalin, U.S. patent No. 2012/0060615 A1 (15 March 2012).
[23]A. H. Hartog and K. Kader, U.S. patent No. 2012/0067118 A1 (22 March 2012).
[24]G. Tu *et al.*, IEEE Photonics Technol. Lett. **27**, 1349 (2015).
[25]A. H. Hartog, O. I. Kotov, and L. B. Liokumovich, *Second EAGE Workshop on Permanent Reservoir Monitoring 2013 – Current and Future Trends* (Stavanger, Norway, 2013).
[26]Y. Shi, H. Feng, and Z. Zeng, Sensors **15**, 21957 (2015).
[27]W. Eickhoff and R. Ulrich, Appl. Phys. Lett. **39**, 693 (1981).
[28]M. Froggatt and J. Moore, Appl. Opt. **37**, 1735 (1998).
[29]D. Zhou, Z. Qin, W. Li, L. Chen, and X. Bao, Opt. Express **20**, 13138 (2012).
[30]M. N. Alahbabi, Y. T. Cho, and T. P. Newson, Opt. Lett. **29**, 26 (2004).
[31]M. N. Alahbabi, N. P. Lawrence, Y. T. Cho, and T. P. Newson, Meas. Sci. Technol. **15**, 1539 (2004).
[32]F. Wang, X. Zhang, X. Wang, and H. Chen, Opt. Lett. **38**, 2437 (2013).
[33]A. Masoudi, M. Belal, and T. P. Newson, Opt. Lett. **38**, 3312 (2013).
[34]T. Kurashima, T. Horiguchi, and M. Tateda, Opt. Lett. **15**, 1038 (1990).
[35]P. Chaube, B. G. Colpitts, D. Jagannathan, and A. W. Brown, IEEE Sens. J. **8**, 1067 (2008).
[36]R. Bernini, A. Minardo, and L. Zeni, Opt. Lett. **34**, 2613 (2009).
[37]Y. Peled, A. Motil, L. Yaron, and M. Tur, Opt. Express **19**, 19845 (2011).
[38]J. Urricelqui, A. Zornoza, M. Sagues, and A. Loayssa, Opt. Express **20**, 26942 (2012).
[39]T. Horiguchi, K. Shimizu, T. Kurashima, M. Tateda, and Y. Koyamada, J. Lightwave Technol. **13**, 1296 (1995).
[40]E. Geinitz, S. Jetschke, U. Ropke, S. Schroter, R. Willsch, and H. Bartelt, Meas. Sci. Technol. **10**, 112 (1999).
[41]L. Thévenaz, S. F. Mafang, and J. Lin, Opt. Express **21**, 14017 (2013).
[42]K. Hotate and M. Tanaka, Photon. Technol. Lett. **14**, 179 (2002).
[43]K. Y. Song and K. Hotate, IEEE Photonics Technol. Lett. **19**, 1928 (2007).
[44]K. Y. Song, M. Kishi, Z. He, and K. Hotate, Opt. Lett. **36**, 2062 (2011).